Contents lists available at ScienceDirect

Chemical Engineering Research and Design

journal homepage: www.elsevier.com/locate/cherd

The impact of model approximation in multiparametric model predictive control

Justin Katz[a,b], *Baris Burnak*[a,b], *Efstratios N. Pistikopoulos*[a,b,*]

[a] *Artie McFerrin Department of Chemical Engineering, Texas A&M University, College Station, TX 77843, USA*
[b] *Texas A&M Energy Institute, Texas A&M University, College Station, TX 77843, USA*

ARTICLE INFO

Article history:
Received 7 August 2018
Received in revised form 18 September 2018
Accepted 20 September 2018
Available online 29 September 2018

Keywords:
Multiparametric programming
Model predictive control
Model validation

ABSTRACT

Incorporating a high fidelity model that accurately describes a dynamical system in a model predictive control study may often lead to an intractable formulation where the use of model approximation is required. This study examines system identification, time series modeling, and linearization in the context of multiparametric model predictive control with the use of key error metrics including: (i) a novel comparison of key features of the feasible space and objective function in the optimization formulation, (ii) integral time absolute error, (iii) error distribution analysis, and (iv) step response profiles. Two examples are used as a basis for this study: a tank system which highlights the techniques used and a Continuously Stirred Tank Reactor (CSTR).

1. Introduction

Model Predictive Control (MPC) is a growing field in the academic and industrial communities for more than three decades now (Camacho and Bordons, 2007; Morari and Lee, 1999; Mayne, 2014). In recent years, more advanced models are being incorporated into these model predictive control frameworks (Santos et al., 2001). The work by Jang et al. (2016) has utilized robust nonlinear model predictive control in the context of a semi-batch polymerization reactor; Albalawi et al. (2017) utilized economic MPC with a catalytic reactor as an example, and Fang and Armaou (2016) has developed nonlinear model predictive control formulations utilizing Carleman approximation.

While direct formulations preserve the dynamics of the high fidelity model, they may result in an intractable, large scale, complex, non-convex optimization problem depending on the complexity of the original model. Problems of this nature can be reduced to tractable forms via model approximation techniques (Diangelakis et al., 2017) that are then incorporated into a model predictive control formulation. Multiparametric programming enables improved online computational effort by providing an offline, explicit solution to the MPC optimization formulation (Bemporad et al., 2002; Oberdieck et al., 2016).

The development of approximate models for model predictive control is pivotal when controlling a complex system. Numerous approximation methods for model predictive control currently exist in the open literature, such as system identification (Ljung, 1999) and linearization around a steady state. These methods are well established and easily implementable with standard softwares, such as the MATLAB System Identification Toolbox™. Recently, advanced techniques using sparse regression, local dynamic decomposition strategies, and Proper Orthogonal Decomposition have been introduced into the literature (Sidhu et al., 2018; Narasingam and Kwon, 2018, 2017; Narasingam et al., 2018). More advanced techniques in the open literature to construct approximate models for MPC applications include Hammerstein-Wiener models (Fruzzetti et al., 1997), feedback linearization (Primbs and Nevistic, 1997; Simon et al., 2013), emperical grammians (Hahn and Edgar, 2002), trajectory linearization (Rewieński and White, 2003; Xie et al., 2011), piecewise linearization (Ozkan et al., 2000), and closed loop re-identification (Kheradmandi and Mhaskar, 2018), at the cost of a more involved procedure, both conceptually and computationally.

* *Corresponding author at:* Artie McFerrin Department of Chemical Engineering, Texas A&M University, College Station, TX 77843, USA.
E-mail address: stratos@tamu.edu (E.N. Pistikopoulos).

https://doi.org/10.1016/j.cherd.2018.09.034
0263-8762/

In tandem with model approximation development, there has been development in model validation via quantitative and qualitative error metrics. Balaguer and Vilanova (2009) has utilized frequency analysis to perform model validation, and Alvarado and Garcia (2018) has extended this approach by incorporating (i) Integral Time Absolute Error (ITAE), (ii) frequency analysis, and (iii) closed loop performance. These error metrics provide confidence in the approximate models developed to be used in control applications.

In the context of multiparametric Model Predictive Control (mpMPC), there has been development in model approximation and validation. Two common model approximation techniques include linearization and system identification (Papathanasiou et al., 2016; Burnak et al., 2018; Diangelakis et al., 2017). A technique introduced by Lambert et al. utilized Monte Carlo based methods to produce an approximate model for mpMPC (Lambert et al., 2013). Recent work in the field of multiparametric model predictive control by Shokry et al. (2016) developed data driven mpMPCs through machine learning techniques. Such model approximations are also at the heart of the PARameteric Optimization and Control (PAROC) framework for the derivation of these explicit/multiparametric controllers (Pistikopoulos et al., 2015). A key question that remains open within the PAROC framework is "what constitutes a suitable approximate model for the derivation of explicit control strategies with multiparametric programming?".

In this work, we introduce novel error metrics based on the optimization formulation of the mpMPCs developed from the approximate models. We present a comprehensive set of error metrics to ascertain the effectiveness of the approximate model via (i) a comparison of the decision space and objective function for the mpMPC formulations, (ii) open loop error metrics comparing the approximate model against the high fidelity model, and (iii) closed loop error metrics in the context of multiparametric model predictive control. Starting with various approximate models developed from standard model approximation techniques, i.e. system identification, time series modeling, and linearization, we construct the mpMPC formulation for each approximate model. These mpMPC formulations are analyzed using the presented set of error metrics, followed by a visual inspection of the closed loop response.

2. Model approximation in multiparametric model predictive control

The development of an affine approximate model for multiparametric programming is a critical step in the PAROC framework within the available algorithms and software for multiparametric programming (Pistikopoulos et al., 2015; Oberdieck et al., 2016). Currently in the open literature, there is no established methodology for ascertaining the "goodness" of the approximate model in the context of control. In the context of multiparametric programming, the dependence of the derived parametric solution on the approximate model has not been fully investigated.

The relationship between the approximate model and a high fidelity model in the context of multiparametric programming is conceptualized as follows. We start with a high fidelity model that is single input with one state, as seen in Eq. (1). The high fidelity model is represented by an approximate model of an affine form, as seen by Eq. (2).

$$\dot{x} = f(x, u), \quad x(0) = x_0 \tag{1}$$

where $x \in \mathbb{R}$ is the state of the system, $u \in U$ is the manipulated action of the system, and f represents the state evolution.

$$x_{t+1} = ax_t + bu_t + c, \quad x(0) = x_0 \tag{2}$$

where x_t is the state of the approximate model at a given time instance, and u is the same as in Eq. (1). The a and b coefficients together with c define this affine approximate model. For clarity, in the following steps c is taken to be zero. The initial state of this system x_0, a, and b are treated as bounded uncertain parameters.

To formulate the optimization problem utilizing the approximate model, Eq. (3) is developed.

$$\begin{aligned}
\min_{u_0} \quad & \sum_{i=1}^{P} x_i^T Q x_i \\
\text{s.t.} \quad & x_{t+1} = ax_t + bu_0, \quad \forall t \\
& x(0) = x_0 \\
& \underline{x} \le x_0 \le \bar{x} \\
& \underline{a} \le a \le \bar{a} \\
& \underline{b} \le b \le \bar{b} \\
& x_t \in X, \quad \forall t \\
& u_0 \in U \\
& t \in [0, 1, \ldots, P]
\end{aligned} \tag{3}$$

where upper and lower bars indicate upper and lower bounds. P is the horizon length, t is the discrete time point, Q is a penalty matrix, and the states and input of the system belong to the set X and U respectively.

Eq. (3) is transformed into a multiparametric programming problem as seen in Eq. (4). The solution to this multiparametric programming problem returns expressions of u as functions of the uncertain parameters, x_0, a, and b. Note, the treatment of a and b as uncertain parameters yields left hand side uncertainty manifesting in the $A(\theta)$ term in Eq. (4). In the general case, the solution to this problem class is still an open question and standard multiparametric techniques are not readily available to solve these problem structures (Khalilpour and Karimi, 2014; Charitopoulos et al., 2017). In the proposed multiparametric problem, Eq. (4), the small scale and low complexity allows us to determine the exact multiparametric solution.

$$\begin{aligned}
u(\theta) = \quad & \underset{u}{\operatorname{argmin}} (Q_{mp}u + H\theta)^T u \\
\text{s.t.} \quad & A(\theta)u \le b_{mp} + F\theta \\
& \theta = [x_0 \quad a \quad b]^T \in \Theta
\end{aligned} \tag{4}$$

where the representative matrices Q_{mp}, H, A, b_{mp}, and F are of appropriate size and are developed by expanding Eq. (2) to the horizon length P and substituting recursively. The bounded uncertain parameters, θ, belong to the set Θ. The solution to this multiparametric programming problem is represented by a collection of critical regions, given in Eq. (5). Inside each critical region belongs a functional representation of the opti-

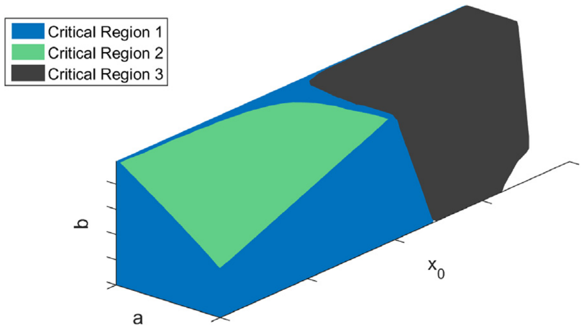

Fig. 1 – The map of solutions for the conceptual example.

mization variable as a function of the uncertain parameters. In this case, the uncertain parameters are the initial condition of the system, x_0, and the coefficients of the approximate model developed, a and b.

The optimal action associated with each critical region is defined in Eq. (5), where Critical Region 1 (CR_1), Critical Region 2 (CR_2), and Critical Region 3 (CR_3) are defined in Appendix A.

$$u = \begin{cases} -\dfrac{a^2(ab+b)+ab}{(ab+b)^2+b^2}x_0, & \text{if } \theta \in CR_1 \\ U_{\max}, & \text{if } \theta \in CR_2 \\ U_{\min}, & \text{if } \theta \in CR_3 \end{cases} \tag{5}$$

The graphical representation of the critical regions for this motivating example is seen in Fig. 1. In the figure, each colored region represents a particular Critical Region with an associated functional relationship between the optimal action, u, and the uncertain coefficients. For instance, the optimal action in Eq. (5) defined by Critical Region 1 is a nonlinear function of the uncertain parameters a and b. To understand this nonlinear effect, consider two instances of a and b realizations in Critical Region 1, namely, (i) $a = 0.5$ and $b = -0.5$, and (ii) $a = 0.2$ and $b = -0.1$. This realization yields to distinct optimal control laws that are affine function of the initial state, as seen by Eq. (6).

$$u(x_0, a = 0.5, b = -0.5) = 0.54x_0 \tag{6a}$$

$$u(x_0, a = 0.2, b = -0.1) = 1.02x_0 \tag{6b}$$

It is evident from Eq. (6) that for the same realization of x_0 in Critical Region 1, the optimal control action would be different.

The benefit of the parametric solution developed is the resulting closed form solution, e.g. Eq. (5), which can be integrated into the high fidelity model, e.g. Eq. (1). The concept of embedding the parametric solution into the high fidelity model has developed into the PAROC framework (Pistikopoulos et al., 2015), represented by Fig. 2. The possibility for the explicit parametric solution to be embedded in the high fidelity model is a key characteristic of mpMPC, and the affine form of the approximate model used is a necessary component in deriving the multiparametric solution.

In this conceptual example, the approximate model was left uncertain, yielding a multiparametric programming problem with left hand side uncertainty. Currently in the open literature, no general solution strategy exists for solving multiparametric programming problems of this type. Therefore, the approximate model used for the mpMPC must be fixed prior to developing the multiparametric solution. Due to the significant effect of the approximate model on the resulting multiparametric solution, it is critical to (i) determine an approximate model that is able to return an effective multiparametric solution, and (ii) detect a priori if the derived approximate model results in an "acceptable" closed loop solution using error metrics.

3. Methodology

This section presents model approximation techniques in conjunction with error metrics to assess multiparametric model predictive controllers.

3.1. *Model based control*

Consider a control policy based on the continuous time high fidelity model, given in Eq. (7). Another control policy, based on a discrete time formulation, customarily described as the conventional model predictive control formulation (Morari and Lee, 1999), is given by Eq. (8).

$$\begin{aligned} \min_{u} \quad & \int_0^{\tau} \left((y - y_{sp})^T QR(y - y_{sp}) + u^T R u \right) dt \\ \text{s.t.} \quad & \dot{x} = f(x, u), \quad x_0 = x(0) \\ & y = h(x, u) \\ & x \in X \\ & y \in Y \\ & u \in U \end{aligned} \tag{7}$$

where QR and R are cost matrices, y_{sp}, y, and x are the set point, output, and states of the high fidelity system respectively. f is a function defining the evolution of the states over time, h defines the relationship between the states of the system and inputs, and u is the input to the high fidelity system. The states, outputs, and inputs belong to the set X, Y, and U respectively. Note, a terminal cost on the final states can be

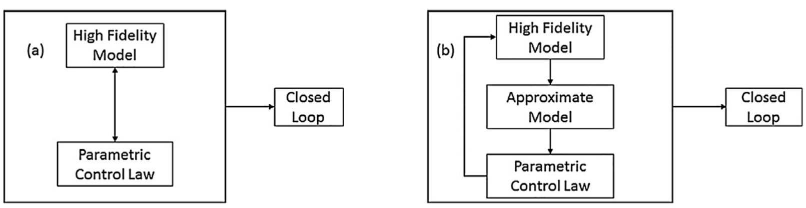

Fig. 2 – (a) Implementation of the ideal case of the general multiparametric solution with the high fidelity model. (b) Implementation of the multiparametric solution derived from the affine approximate model with the high fidelity model.

Table 1 – The vertices defining the polytope in Eq. (13).

Vertex ID	u	θ
1	0.1	0.2
2	0.9	0.2
3	0.5	0.8

incorporated in the objective function but is not included in this formulation for brevity.

$$\begin{aligned}
\min_{u_0,\ldots,u_{NC}} \quad & \sum_{i=1}^{OH}(y_i-y_{sp})^T QR(y_i-y_{sp})+\sum_{i=0}^{NC}u_i^T Ru_i\\
\text{s.t.} \quad & x_{t+1}=Ax_t+Bu_t, \quad \forall t\\
& y_t=Cx_t+Du_t, \quad \forall t>0\\
& u_t=u_{NC}, \quad \forall t>NC\\
& x_0=x(0)\\
& y_t\in Y, \quad \forall t>0\\
& u_t\in U, \quad \forall t\\
& t\in[0,1,\ldots,OH]
\end{aligned} \tag{8}$$

where A, B, C, and D are the associated state space matrices. The states of the approximate system are x, the estimated outputs are y, OH is the output horizon of the system and NC is the control horizon of the system where $NC \le OH$. The outputs of the system, y, belong to the set Y and are predictions of the high fidelity output. All other terms are the same as in Eq. (7).

Due to the approximation of the high fidelity model, the output of the approximate model in Eq. (8) is not guaranteed to follow the real output of the system in Eq. (7). To account for this mismatch, a mismatch term is added to the MPC formulation in the form of Eq. (9) (Ziogou et al., 2013).

$$e=y_{real}-y_0 \tag{9}$$

where y_{real} is the real system output, y is the approximate output, and e is the associated error.

Eq. (8) is transformed to a multiparametric MPC which can be solved explicitly offline to determine the optimal control action as an affine function of the uncertain parameters, namely the initial state of the system and the set point. Details regarding the transformation of the MPC problem to an mpMPC problem are in the open literature (Bemporad et al., 2002; Pistikopoulos et al., 2002; Kouramas et al., 2011; Takács and Rohal'-Ilkiv, 2012).

3.2. Model approximation

In this work, the development of an affine approximate model used in the multiparametric formulation is mandatory. Many techniques exist in the open literature in deriving approximate models in this form such as a emperical grammians or dynamic mode decomposition with control (Narasingam and Kwon, 2017). In this work, a representative set of approximate model techniques are employed to explore (i) determining an approximate model that returns an effective multiparametric solution, and (ii) determine a priori if the developed approximate model yields "acceptable" closed loop results via suitable error metrics. To this end, the model approximation techniques used are system identification, time series models, and first order Taylor approximation. System identification and time series modeling are data based techniques where the MATLAB System Identification Toolbox™ is used to develop the relevant models. Developing these models requires input/output data.

Table 2 – Error metric results for the tank example, where DSV is decision space volume, OL is open loop, and CL is closed loop.

	Linear	System Id	BJ	ARX	OE
DSV	0.63	1	0.59	0.61	0.58
L^2 norm	4.8e3	4.9e3	4.8e3	4.9e3	4.7e3
ITAE OL	163	243	288	653	527
ITAE CL (10^3)	3.6	2.9	2.9	2.3	2.4
Step Resp	✓	✓	✓	✓	✓

To generate an input signal, a Pseudo Random Binary Sequence (PRBS) is used. The choice of the input signal used is to ensure proper excitation of the underlying high fidelity system. Following generation of the PRBS input signal, the output data is generated by passing the input signal to the high fidelity model. The developed approximate models from the input/output data are used to approximate the f and h functions in Eq. (7). A brief review of these data driven techniques is discussed in the following subsections.

3.2.1. System identification

System identification is a technique based on input/output data which results in a discrete time state space model (Ljung, 1999). The form of the equation is presented in Eq. (10).

$$x_{t+1}=Ax_t+Bu_t \tag{10a}$$

$$y_t=Cx_t+Du_t \tag{10b}$$

where the matrices A, B, C, and D are the state space matrices that define the evolution of the states. The states of the approximate model are x, u is the manipulated input to the system, and y is the predicted output of the system. It is important to note that the states developed from system identification are pseudostates and do not hold physical meaning.

3.2.2. Time series modeling

Time series models develop a model structure to predict future outputs based on previous outputs and inputs. The general structure for time series models is seen by Eq. (11).

$$A(q)y(t)=\frac{B(q)}{F(q)}u(t)+\frac{C(q)}{D(q)}e(t) \tag{11}$$

where y is the predicted output, e is the error, u is the manipulated input to the system, and q is the delay operator, and the matrices A, B, F, C, and D define the time series model structure (Ljung, 1999). This model structure can be converted into a state space representation to be used in an MPC formulation (Jørgensen et al., 2011). The classes of time series models used are Box-Jenkins (BJ), Output Error (OE), and AutoRegressive eXogenous (ARX).

3.3. Error metrics

The error metrics used in this work fall under three categories, (i) error metrics associated with the optimization formulation, (ii) open loop error metrics, and (iii) closed loop error metrics. These three classes are discussed in the subsequent subsections.

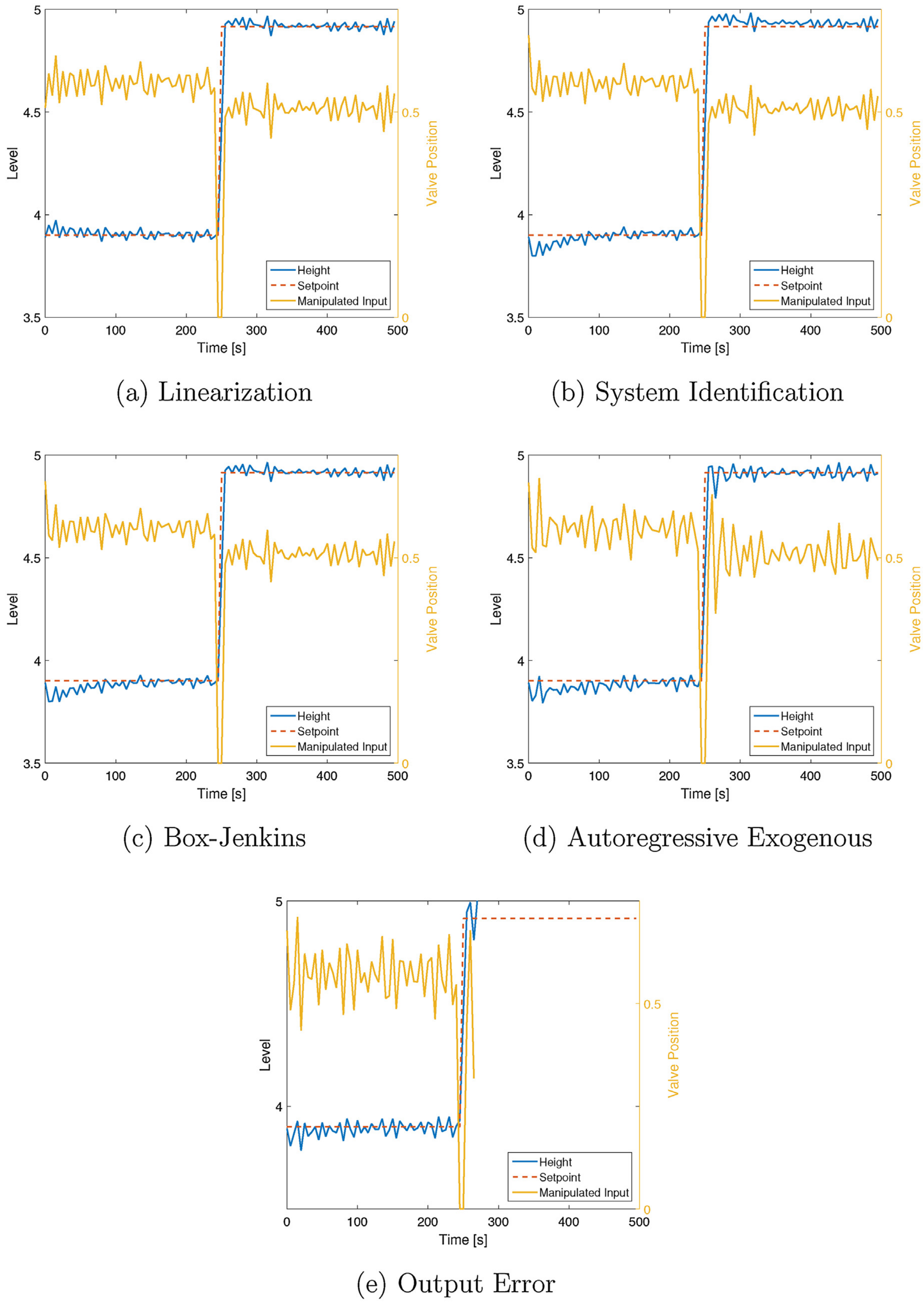

(a) Linearization (b) System Identification (c) Box-Jenkins (d) Autoregressive Exogenous (e) Output Error

Fig. 3 – Closed loop response of the different model approximations. The manipulated action corresponds to the right y-axis.

3.3.1. *Optimization formulation error metrics*

Established approaches to model validation assess the approximate model in the context of open loop or closed loop performance. In this study, we present novel error metrics focusing on the optimization formulation developed via the approximate model. Two key components of the approximate and high fidelity optimization formulations are compared, namely their (i) decision space and (ii) objective function.

3.3.1.1. *Decision space volume comparison.* The proposed metric calculates the feasible space volume projected on its decision space. The decision space volume is calculated for

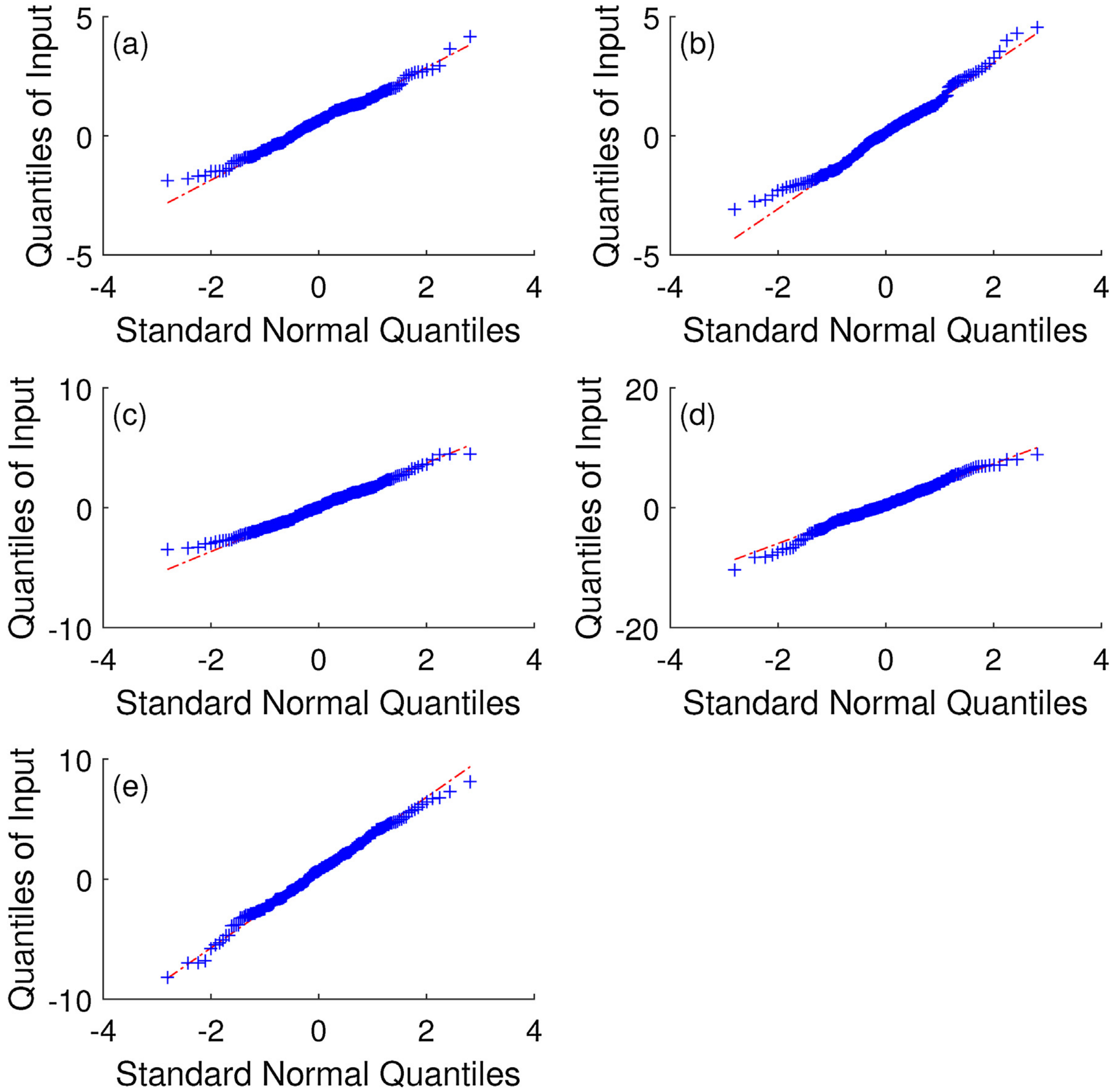

Fig. 4 – Q–Q plot for the open loop comparison where (a) is linearization, (b) is system identification, (c) is Box–Jenkins, (d) is autoregressive exogenous, and (e) is output error.

each mpMPC developed from the various approximate models as a quantitative test for the degree of freedom for each controller. Smaller decision space volumes indicate an mpMPC that is more restricted in the selection of the optimal control action. The procedure for calculating the decision space volume is described as follows. A representative feasible space for an mpMPC is defined by Eq. (12).

$$Au \leq b + F\theta \tag{12}$$

In Eq. (12), u is the control action, θ is the uncertain parameter, and A, b, and F are the associated matrices of the feasible space. The vertices of the polytope associated with Eq. (12) are determined to calculate the decision space volume. The dimensionality of the decision space volume depends on the control horizon and number of manipulated actions because they directly affect the number of optimization (decision) variables. This is apparent from the length of the vector u, which is equal to the number of manipulated actions multiplied by the control horizon. Thus an increase in either the manipulated actions or the control horizon increases the dimensionality of the decision space volume.

The procedure for the decision space volume calculation is conceptualized as follows. Consider a feasible region defined by Eq. (13).

$$0 \leq u \leq 1 \tag{13a}$$

$$0 \leq \theta \leq 1 \tag{13b}$$

$$0.6\theta - 0.8u \leq 0.03 \tag{13c}$$

$$-\theta \leq -0.2 \tag{13d}$$

$$0.8u + 0.6\theta \leq 0.9 \tag{13e}$$

The vertices defining the polytope in Eq. (13) are shown in Table 1. The bounds of u are bounded between 0 and 1, however, from Table 1 it is seen that the maximum and minimum attainable u values are 0.9 and 0.1, respectively. Therefore, the decision space volume is the difference between these maximum and minimum attainable bounds for u and is 0.8.

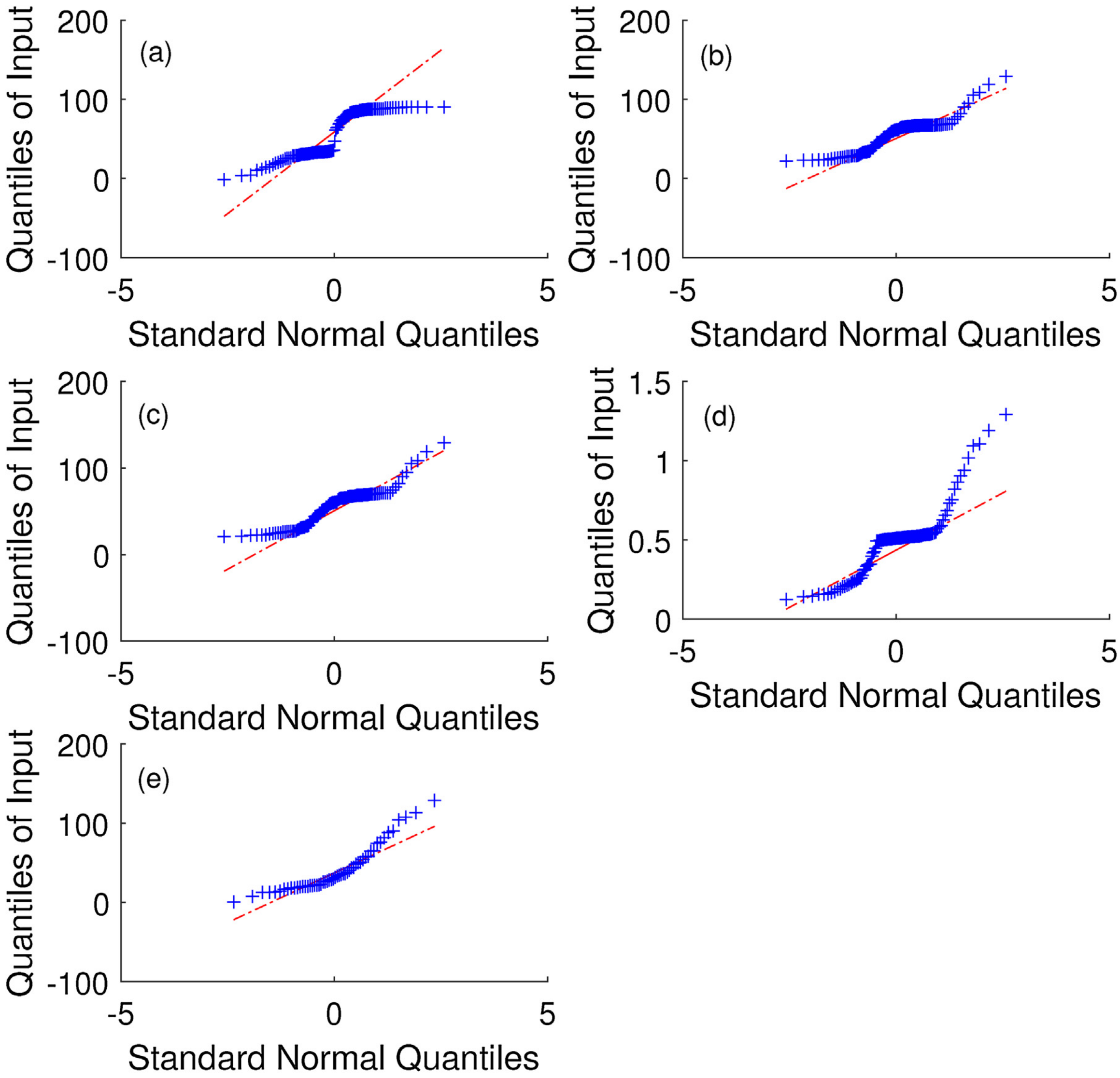

Fig. 5 – Q–Q plot comparison for the closed loop tank example where (a) is linearization, (b) is system identification, (c) is Box–Jenkins, (d) is autoregressive exogenous, and (e) is output error.

3.3.1.2. *Objective function comparison*. The construction of the objective function from the approximate model is validated via a function error norm. The L^2 function norm is taken between the objective function constructed from the high fidelity model (i.e. Eq. (7)) and the objective function constructed from the approximate model (i.e. Eq. (8)), as seen in Eq. (14).

$$||J - g||^2 = \int_X |J - g|^2 \, dx \tag{14}$$

where J and g are the high fidelity and approximate objective function respectively. For example, if the objective function in Eq. (8) was expanded for a given prediction horizon using Eq. (10), g would correspond to the objective function seen in Eq. (15).

$$g = (C(Ax_0 + Bu_0) + Du_0 - y_{sp})^T QR(C(Ax_0 + Bu_0) + Du_0 - y_{sp}) + u_0^T Ru_0 + \cdots \tag{15}$$

The L^2 function norm provides a quantitative analysis regarding the proximity of the two objective functions. Data driven techniques are available to calculate the potentially high dimensional integral given by Eq. (14). One common method is to employ Monte Carlo methods (Stefan Weinzierl, 2000). Also, the occurrence of physically meaningless pseudostates from the use of data driven techniques presents a dimensionality mismatch between J and g. While the output of these objective functions is scalar, the input to each objective function is different and therefore returns a dimensionality mismatch. To ensure proper input dimensionality when evaluating the L^2 function norm, the pseudostates are fixed to their initial conditions developed during their construction.

3.3.2. *Open loop error metrics*

Standard open loop error metrics are employed to develop confidence in the approximate models. These error metrics provide both quantitative and qualitative analysis of the resulting approximate models. Three open loop error metrics are utilized in this work: (i) the step response profile, (ii) ITAE, and (iii) a distribution analysis.

3.3.2.1. *Step response profiles*. Step response profiles show the output of the system for a step in the input. It provides a qualitative measure regarding the system of interest to each input.

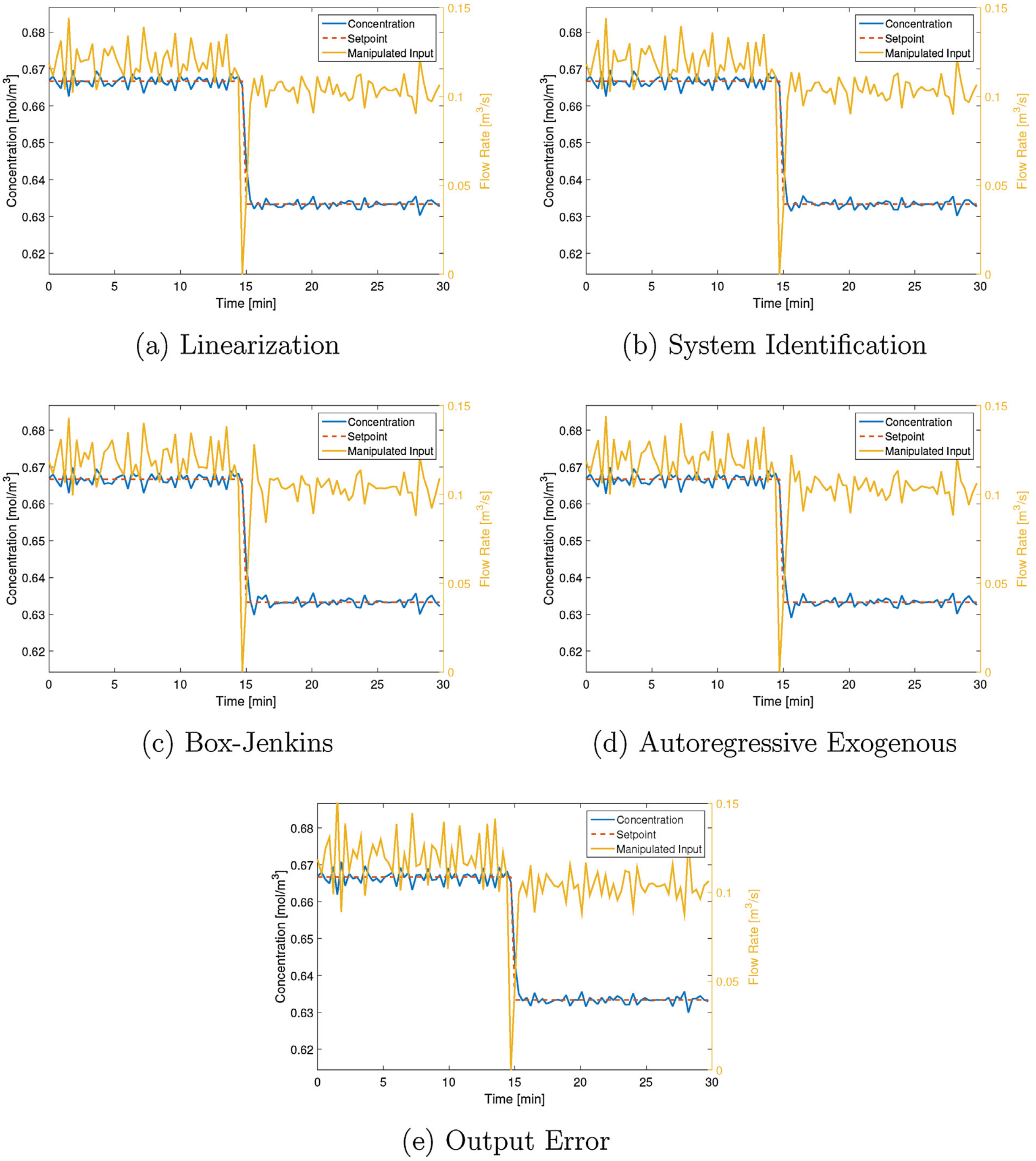

(a) Linearization

(b) System Identification

(c) Box-Jenkins

(d) Autoregressive Exogenous

(e) Output Error

Fig. 6 – Closed loop response of the different model approximations. The manipulated action corresponds to the right y-axis.

This is a property that is inherent with the high fidelity model, and the approximate model sharing this property provides reassurance that the input/output relationship is preserved. Verifying that the approximate model steps in the same manner as the high fidelity model is shown by a yes (✓) or no (×).

3.3.2.2. *Integral Time Absolute Error (ITAE)*. The ITAE is used to validate the open loop performance of the approximate model with the high fidelity model, as seen in Eq. (16).

$$ITAE = \Sigma i|e_i| \quad (16)$$

where i is the sample index and e_i is the error of the *ith* sample. As the error term remains nonzero for longer sample times, the ITAE value increases at a faster rate. The lower the value of the ITAE, the better the approximate model is at representing the high fidelity model.

3.3.2.3. *Error distribution analysis*. A qualitative test via a Q–Q plot compares the error between the approximate and high fidelity model output to the noise distribution applied to the system. Data that resembles a line indicates no difference between the error and the noise distribution applied to the system.

3.3.3. *Closed loop error metrics*

The error metrics used for the closed loop performance are ITAE and analyzing the closed loop error distribution. The details regarding these metrics are defined in Section 3.3.2.

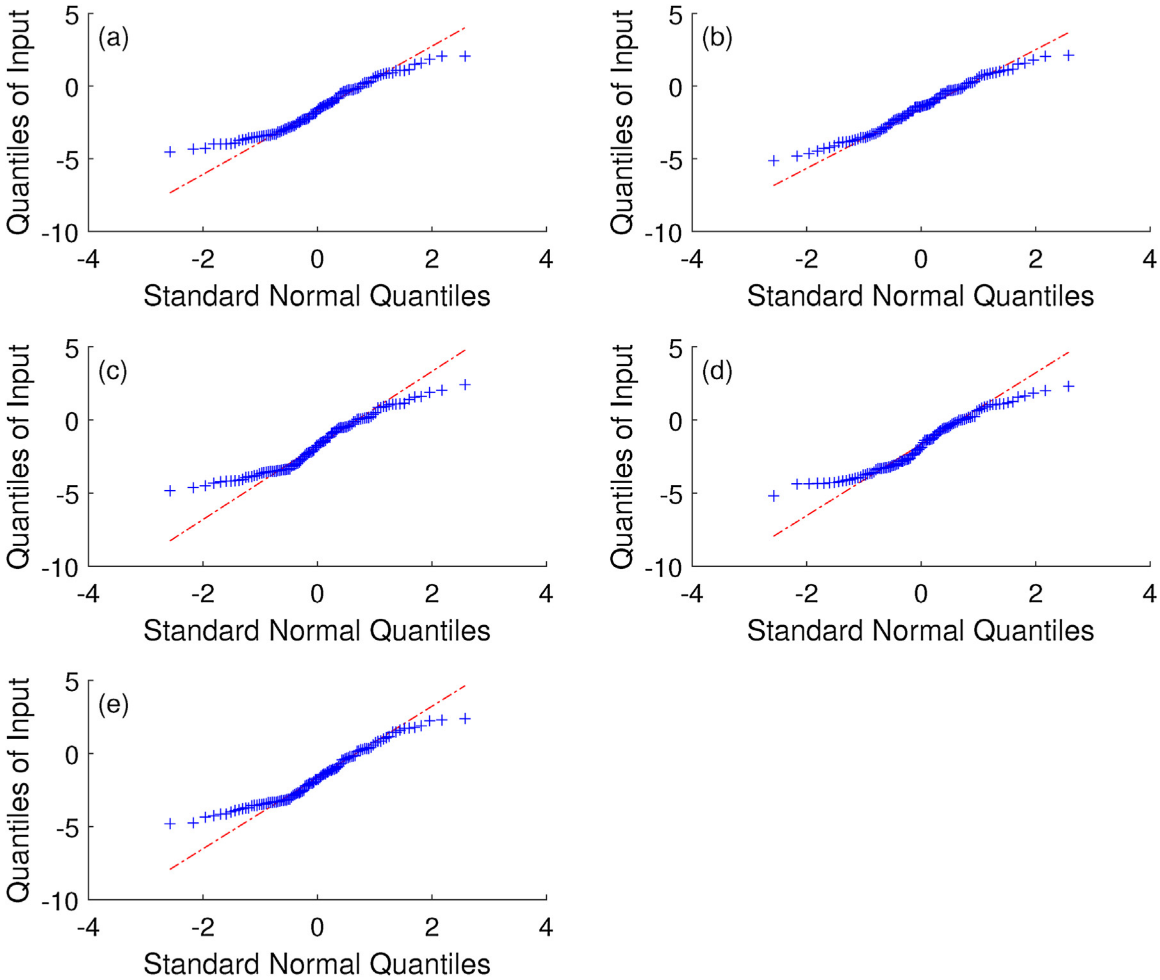

Fig. 7 – Q–Q plot comparison for the closed loop CSTR example where (a) is linearization, (b) is system identification, (c) is Box–Jenkins, (d) is autoregressive exogenous, and (e) is output error.

Table 3 – Error metric results for the CSTR example, where DSV is decision space volume, OL is open loop, and CL is closed loop.

α		Linear	System Id	BJ	ARX	OE
1	DSV	0.31	0.67	0.31	0.31	0.33
	L^2 norm	319	348	351	342	352
	Q–Q OL	√	√	√	√	√
	ITAE OL	19	25	21	28	26
	ITAE CL	13	12	14	13	13
	Step Resp	√	√	√	√	√
2	DSV	0.33	0.85	0.79	0.34	0.35
	L^2 norm	288	291	296	296	290
	Q–Q OL	√	√	√	√	√
	ITAE OL	18	20	20	19	21
	ITAE CL	18	18	19	19	19
	Step Resp	√	√	√	√	√
3	DSV	0.35	1	1	0.35	0.35
	L^2 norm	289	274	268	273	266
	Q–Q OL	√	√	√	√	√
	ITAE OL	17	16	22	17	19
	ITAE CL	24	23	12	23	23
	Step Resp	√	√	√	√	√

4. Examples

4.1. *Level tracking of a tank*

We present a motivating example to demonstrate the proposed error metrics and the model approximation techniques used. The tank has a fixed inlet flow and the flow out of the tank is manipulated via a valve on the exit of the tank. The control objective of the system is to maintain the level of the tank at a specified target. The system maintains a nonlinearity in the form of a square root, as seen in Eq. (17).

$$\frac{dh}{dt} = \frac{F}{A} - u\sqrt{2gh}\frac{A_{out}}{A} \tag{17}$$

The manipulated variable, u, maintains bounds between 0 and 1. The state of the system, h (m), must remain nonnegative. The parameters g (m/s^2), A (m^2), and A_{out} (m^2) are gravity, the area of the tank, and the outlet area of the tank respectively. Eq. (17) is approximated using the model approximation techniques discussed in Section 3 to develop the corresponding MPC, based on Eq. (8). For this example, the penalty on the manipulated action, R, is taken to be zero.

The approximate models and resulting mpMPC are developed for each model approximation technique. The control objective is to track a set point while the output signal is affected by noise with a magnitude of 1% of the steady state value to ensure consistency between the different closed loop profiles. The number of critical regions the developed multiparametric controllers have range from 10 to 500 and are available at http://paroc.tamu.edu/. Halfway through the simulation, the set point is step changed to a new value to test the mpMPC under a transition and at different operating conditions. The error metrics used are summarized in Table 2, where a check mark (√) indicates good performance for qual-

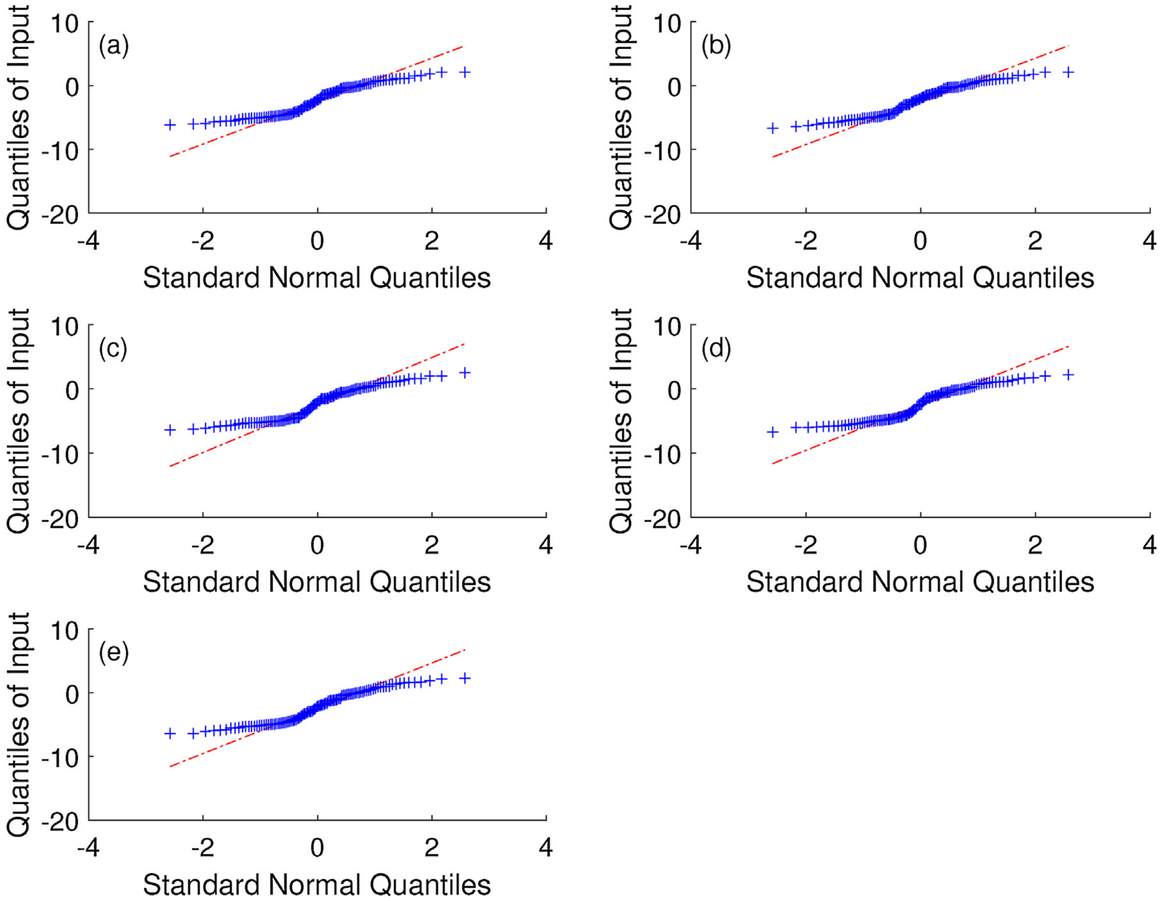

Fig. 8 – Q–Q plot for the closed loop comparison of an α of 2 where (a) is linearization, (b) is system identification, (c) is Box–Jenkins, (d) is autoregressive exogenous, and (e) is output error.

itative metrics. First, the open loop ITAE indicates under open loop testing the approximate models are able to identify with the high fidelity model at different calibers. Second, the closed loop ITAE is opposite to the open loop case, where linearization has the highest closed loop ITAE and ARX has the lowest closed loop ITAE. The difference between the open and closed loop ITAE is evidence that open loop testing is inadequate for assessing the closed loop performance. The optimization formulation error metrics show two key points. The first point is that all approximate models have similar L^2 norm values against the high fidelity model, indicating similar closed loop performance, validated qualitatively from Fig. 3. However, the decision space volume shows clear discrepancies between the approximate models. The mpMPC developed from system identification has the largest decision space and the mpMPC developed from OE has the smallest decision space. The smaller decision space provides less degrees of freedom for the controller to operate in causing potential controller failure, as seen in Fig. 3(e) which is the closed loop profile for the mpMPC developed based on the OE approximate model. Looking at the original bounds of the decision space, the manipulated action is bounded between 0 and 1, therefore, the decision space volume is 1. As seen by Table 2, approximately a 40% reduction in the decision space is seen from the approximate formulations developed from linearization, BJ, ARX, and OE. However, the approximate formulation developed from system identification maintains the full decision space volume. The closed loop performance is presented in Fig. 3. From the closed loop response, all of the approximate models, except for OE, are capable of tracking the given set point under a noisy output signal. The closed loop performance of the mpMPC developed from OE results in a simulation that violates the upper bound of the process.

The open and closed loop Q–Q plots used as a qualitative metric are developed from the error between the approximate model output and the noisy output from the high fidelity model, and are seen from Figs. 4 and 5. Therefore, let us denote the output of the approximate model as $\hat{y}$, the output from the high fidelity model as $\bar{y}$, and the noise affecting the output signal as η, then the difference between the approximate model and high fidelity model output is $\bar{y} + \eta - \hat{y}$. If the approximate model perfectly matches the high fidelity model, then the error between the approximate and high fidelity model is the noisy signal (η), otherwise it is a result of the plant model mismatch. Since the noisy signal is developed from a normal random distribution, the Q–Q plot provides evidence if the error is similar to a normal distribution, or if it is affected by plant model mismatch. Fig. 4 reveals that all of the approximate models in open loop are able to accurately represent the high fidelity model, as seen by the data points conforming to the straight line in the figure. The closed loop Q–Q plot, given by Fig. 5, shows that all of the approximate models are affected by plant model mismatch. However, portions of the closed loop Q–Q plot show linear trends providing evidence that the approximate model is able to match the high fidelity model.

4.2. *Continuously Stirred Tank Reactor*

A single reaction, isothermal, and constant volume Continuously Stirred Tank Reactor (CSTR) is considered. To increase

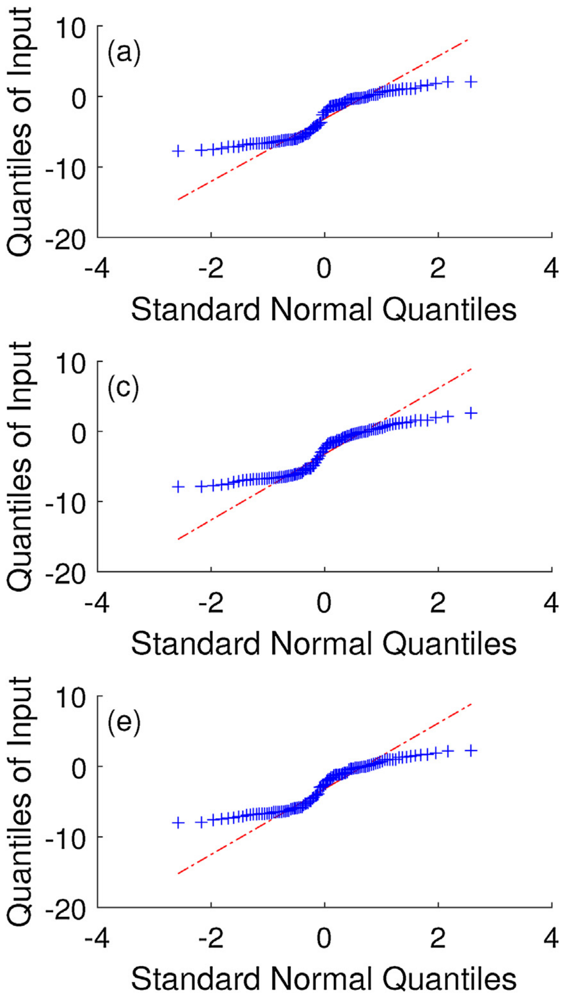

Fig. 9 – Q–Q plot for the closed loop comparison of an α of 3 where (a) is linearization, (b) is system identification, (c) is Box–Jenkins, (d) is autoregressive exogenous, and (e) is output error.

the complexity of the high fidelity model, the reaction order is increased from first order through third order under the same analysis. The CSTR has an adjustable flow rate of reactant into the reactor. The control objective for this example problem is to maintain a specified reactant concentration level in the reactor while minimizing the use of the reactant flow.

$$\frac{dC_A}{dt} = \frac{F}{V}(C_{A_i} - C_A) - kC_A^{\alpha} \tag{18a}$$

$$\frac{dC_B}{dt} = \frac{F}{V}(-C_B) + kC_A^{\alpha} \tag{18b}$$

The mass balance for the system is described by Eq. (18), where the amount of reactant and product vary based on the inlet flow and the reaction mechanism. The manipulated flow into the reactor, F (m^3/s), is bounded between 0 and 1, and the states of the system, the reactant (C_A) and product (C_B) concentration (mol/m^3), are also bounded between 0 and 1. V (m^3) is the volume of the system, k is the rate constant of the system, C_{A_i} is the inlet reactant concentration, and the system order is α, taking a value of either 1, 2, or 3. The MPC formulation for this example problem includes set point tracking and is determined for a steady state operating point. At this operating point, there is an exact mapping between the reactant and product concentrations, thus the reactant concentration set point is used, and corresponds to the product concentration set point of interest. There is also a nonzero R term in the objective function, seen in Eq. (8), to penalize usage of the reactant material.

The approximate models and resulting mpMPC are developed for each model approximation technique. The control objective is to track a set point while the output signal is affected by noise, similar to the tank example, and to penalize usage of the manipulated action. The number of critical regions the developed multiparametric controllers have range from 10 to 500 and are available at http://paroc.tamu.edu/. The set point is changed halfway through the simulation for the same reasons as in the tank example. Due to the plethora of figures generated, only an α value of 1 is considered in this section, closed loop Q–Q plots regarding α values of 2 and 3 can be found in Appendix A. The closed loop performance is presented in Fig. 6. From the closed loop response, all of the approximate models are capable of tracking the given set point. The open loop, closed loop, and optimization formulation error criteria are summarized in Table 3 and Fig. 7.

The open loop Q–Q plots reveal that all of the approximate models in open loop are able to accurately represent the high fidelity model, shown by the check mark in Table 3. The closed loop Q–Q plots, given by Fig. 7, show that all of the approximate models conform to a straight line, but are still affected by plant model mismatch.

The key points in Table 3 are summarized as follows: (i) increasing α causes an increase in the closed loop ITAE for all approximate models, (ii) all of the approximate models have similar L^2 norms indicating similar closed loop performance, as verified by the closed loop ITAE and Fig. 3, and (iii) the decision space volume is similar among two groups of approximate models: (1) linearization, ARX, and OE, and (2) system identified and BJ.

5. Conclusions

In this work we presented novel error metrics, based on the decision space volume and objective function comparisons, and standard error metrics that were used to provide confidence in approximate models used in multiparametric model predictive control. These error metrics were used in open loop, closed loop, and on the resulting optimization formulation developed. A tank and CSTR with varying reaction order were examined with the use of these error metrics along with multiparametric model predictive controllers to ascertain the effectiveness of the proposed metrics.

The optimization formulation based error metrics presented account for the decision space volume and differences between objective functions. The decision space volume provides a metric for the manipulated variables in the optimization formulation and the objective function comparison provides a distance metric for the different objective functions. However, information regarding the output space, location of the feasible space, and the effect of pseudostates all play a key role in the closed loop performance. Future directions would incorporate these topics to improve the current analysis.

Acknowledgements

We acknowledge the financial support from the NSF (Grant no. 1705423), under the project titled SusChEM: An integrated framework for process design, control and scheduling [PAROC].

Appendix A.

The regions CR_1, CR_2, and CR_3 are defined as follows.

$$CR_1 = \begin{cases} -\dfrac{2X_{\max} + 2X_{\max}a - ax_0 + Xmaxa^2 - a^2x_0}{a^2+2a+2} \leq 0 \\ \dfrac{2X_{\min} + 2X_{\min}a - ax_0 + X_{\min}a^2 - a^2x_0}{a^2+2a+2} \leq 0 \\ -\dfrac{2X_{\max} + 2X_{\max}a + ax_0 + X_{\max}a^2}{a^2+2a+2} \leq 0 \\ \dfrac{2X_{\min} + 2X_{\min}a + ax_0 + X_{\min}a^2}{a^2+2a+2} \leq 0 \\ -U_{\max} - \dfrac{2a^2(b+ab)+2ab}{2((b+ab)^2+b^2)}x_0 \leq 0 \\ U_{\min} + \dfrac{2a^2(b+ab)+2ab}{2((b+ab)^2+b^2)}x_0 \leq 0 \end{cases}$$

$$CR_2 = \begin{cases} 2Qx_0a^3b + 2QU_{\max}a^2b^2 + 2Qx_0a^2b + 4QU_{\max}ab^2 \\ \quad +2Qx_0ab + 4QU_{\max}b^2 \leq 0 \\ U_{\max}b - X_{\max} + ax_0 \leq 0 \\ X_{\min} - U_{\max}b - ax_0 \leq 0 \\ a^2x_0 - X_{\max} + U_{\max}(b+ab) \leq 0 \\ X_{\min} - a^2x_0 - U_{\max}(b+ab) \leq 0 \end{cases}$$

$$CR_3 = \begin{cases} -(2Qx_0a^3b + 2QU_{\min}a^2b^2 + 2Qx_0a^2b + 4QU_{\min}ab^2 \\ \quad +2Qx_0ab + 4QU_{\min}b^2) \leq 0 \\ U_{\min}b - X_{\max} + ax_0 \leq 0 \\ X_{\min} - U_{\min}b - ax_0 \leq 0 \\ a^2x_0 - X_{\max} + U_{\min}(b+ab) \leq 0 \\ X_{\min} - a^2x_0 - U_{\min}(b+ab) \leq 0 \end{cases}$$

References

Albalawi, F., Durand, H., Christofides, P.D., 2017. Distributed economic MPC with safety-based constraints for nonlinear systems. IFAC-PapersOnLine 50 (1), 12033–12040.
Alvarado, C.S.M., Garcia, C., 2018. Comparison of statistical metrics and a new fuzzy method for validating linear models used in model predictive control controllers. Ind. Eng. Chem. Res. 57 (10), 3666–3677.
Balaguer, P., Vilanova, R., 2009. Frequency-dependent approach to model validation for iterative identification and control schemes. IET Control Theory Appl. 3 (1), 98–109.
Bemporad, A., Morari, M., Dua, V., Pistikopoulos, E.N., 2002. The explicit linear quadratic regulator for constrained systems. Automatica 38, 3–20.
Burnak, B., Katz, J., Diangelakis, N.A., Pistikopoulos, E.N., 2018. Simultaneous process scheduling and control: a multiparametric programming-based approach. Ind. Eng. Chem. Res. 57 (11), 3963–3976.
Camacho, E.F., Bordons, C., 2007. Nonlinear Model Predictive Control: An Introductory Review. Springer, Berlin, Heidelberg, pp. 1–16.
Charitopoulos, V.M., Papageorgiou, L.G., Dua, V., 2017. Multi-parametric linear programming under global uncertainty. AIChE J. 63 (9), 3871–3895.
Diangelakis, N.A., Burnak, B., Katz, J., 2017. Process design and control optimization: a simultaneous approach by multi-parametric programming. AIChE J.
Fang, Y., Armaou, A., 2016. Carleman approximation based quasi-analytic model predictive control for nonlinear systems. AIChE J. 62 (11), 3915–3929.
Fruzzetti, K.P., Palazoğlu, A., McDonald, K.A., 1997. Nolinear model predictive control using Hammerstein models. J. Process Control 7 (1), 31–41.
Hahn, J., Edgar, T.F., 2002. An improved method for nonlinear model reduction using balancing of empirical gramians. Comput. Chem. Eng. 26, 1379–1397.
Jørgensen, J.B., Huusom, J.K., Rawlings, J.B., 2011. Finite horizon MPC for systems in innovation form. 50th IEEE Conference on Decision and Control and European Control Conference, 1896–1903.
Jang, H., Lee, J.H., Biegler, L.T., 2016. A robust NMPC scheme for semi-batch polymerization reactors. IFAC-PapersOnLine 49 (7), 37–42.
Khalilpour, K., Karimi, I., 2014. Parametric optimization with uncertainty on the left hand side of linear programs. Comput. Chem. Eng. 60, 31–40.
Kheradmandi, M., Mhaskar, P., 2018. Model predictive control with closed-loop re-identification. Comput. Chem. Eng. 109, 249–260.
Kouramas, K.I., Faísca, N.P., Panos, C., Pistikopoulos, E.N., 2011. Explicit/multi-parametric model predictive control (MPC) of linear discrete-time systems by dynamic and multi-parametric programming. Automatica 47 (8), 1638–1645.
Lambert, R.S.C., Rivotti, P., Pistikopoulos, E.N., 2013. A Monte-Carlo based model approximation technique for linear model predictive control of nonlinear systems. Comput. Chem. Eng. 54, 60–67.
Ljung, L., 1999. System Identification Theory for the User. Prentice-Hall, EngleWood Cliffs, NJ.

Mayne, D.Q., 2014. Model predictive control: recent developments and future promise. Automatica 50 (12), 2967–2986.
Morari, M., Lee, J.H., 1999. Model predictive control: past, present and future. Comput. Chem. Eng. 23 (4), 667–682.
Narasingam, A., Kwon, J.S.-I., 2017. Development of local dynamic mode decomposition with control: application to model predictive control of hydraulic fracturing. Comput. Chem. Eng. 106, 501–511.
Narasingam, A., Kwon, J.S.-I., 2018. Data-driven identification of interpretable reduced-order models using sparse regression. Comput. Chem. Eng.
Narasingam, A., Siddhamshetty, P., Kwon, J.S.-I., 2018. Handling spatial heterogeneity in reservoir parameters using proper orthogonal decomposition based ensemble Kalman filter for model-based feedback control of hydraulic fracturing. Ind. Eng. Chem. Res. 57 (11), 3977–3989.
Oberdieck, R., Diangelakis, N.A., Papathanasiou, M.M., Nascu, I., Pistikopoulos, E.N., 2016. POP – Parametric Optimization Toolbox. Ind. Eng. Chem. Res. 55, 8979–8991.
Ozkan, L., Kothare, M.V., Georgakis, C., 2000. Model predictive control of nonlinear systems using piecewise linear models. Comput. Chem. Eng. 24, 793–799.
Papathanasiou, M.M., Avraamidou, S., Oberdieck, R., Mantalaris, A., Steinebach, F., Morbidelli, M., Mueller-Spaeth, T., Pistikopoulos, E.N., 2016. Advanced control strategies for the multicolumn countercurrent solvent gradient purification process. AIChE J. 62, 2341–2357.
Pistikopoulos, E.N., Dua, V., Bozinis, N.A., Bemporad, A., Morari, M., 2002. On-line optimization via off-line parametric optimization tools. Comput. Chem. Eng. 26 (2), 175–185.
Pistikopoulos, E.N., Diangelakis, N.A., Oberdieck, R., Papathanasiou, M.M., Nascu, I., Sun, M., 2015. PAROC—An integrated framework and software platform for the optimisation and advanced model-based control of process systems. Chem. Eng. Sci. 136, 115–138.
Primbs, J.A., Nevistic, V., 1997. MPC extensions to feedback linearizable systems. Proceedings of the American Control Conference, 2073–2077.
Rewieński, M., White, J., 2003. A trajectory piecewise-linear approach to model order reduction and fast simulation of nonlinear circuits and micromachined devices. IEEE Trans. Comput.-Aided Design Integr. Circuits Syst. 22 (2), 155–170.
Santos, L.O., Afonso, P.A.F.N.A., Castro, J.A.A.M., Oliveira, N.M.C., Biegler, L.T., 2001. On-line implementation of nonlinear mpc: an experimental case study. Control Eng. Pract. 9 (8), 847–857.
Shokry, A., Dombayci, C., Espuña, A., 2016. Multiparametric metamodels for model predictive control of chemical processes. Comput. Aided Chem. Eng. 38, 937–942.
Sidhu, H.S., Narasingam, A., Siddhamshetty, P., Kwon, J.S.-I., 2018. Model order reduction of nonlinear parabolic PDE systems with moving boundaries using sparse proper orthogonal decomposition: application to hydraulic fracturing. Comput. Chem. Eng. 112, 92–100.
Simon, D., Lofberg, J., Glad, T., 2013. Nonlinear model predictive control using feedback linearization and local inner convex constraint approximations. Proceedings of the 2013 European Control Conference, 2056–2061.
Weinzierl, S., 2000. Introduction to Monte Carlo methods. Technical report.
Takács, G., Rohal'-Ilkiv, B., 2012. Basic MPC Formulation. Springer, London, pp. 207–251.
Xie, W., Bonis, Y., Theodoropoulos, C., 2011. Off-line model reduction for on-line linear MPC of nonlinear large-scale distributed systems. Comput. Chem. Eng. 35, 750–757.
Ziogou, C., Pistikopoulos, E.N., Georgiadis, M.C., Voutetakis, S., Papadopoulou, S., 2013. Empowering the performance of advanced NMPC by multiparametric programming—an application to a PEM fuel cell system. Ind. Eng. Chem. Res. 52 (13), 4863–4873.